Aquaculture 433 (2014) 325–334

Contents lists available at ScienceDirect

Aquaculture

journal homepage: www.elsevier.com/locate/aqua-online

Molecular identification of a new androgenic gland-specific insulin-like gene from the mud crab, *Scylla paramamosain*

Yaqun Zhang [a,1], Kun Qiao [a,1], Shuping Wang [a], Hui Peng [a,b], Zhongguo Shan [a], Kejian Wang [a,b,*]

[a] State Key Laboratory of Marine Environmental Science, Xiamen University, Xiamen 361102, PR China
[b] Marine Biological Preparation Technology Engineering Laboratory of Fujian, Center for Marine Biotechnology, College of Ocean and Earth Sciences, Xiamen University, Xiamen 361102, PR China

ARTICLE INFO

Article history:
Received 15 February 2014
Received in revised form 14 June 2014
Accepted 25 June 2014
Available online 1 July 2014

Keywords:
The androgenic gland
Sex differentiation
Scylla paramamosain
Endocrine
Insulin-like gene

ABSTRACT

It is well known that the androgenic gland is a specific endocrine organ of the male crustacean, controlling its primary and secondary sexual characteristics. The androgenic gland hormone is a key peptide hormone involved in sexual differentiation in crustaceans. In this study, a full length cDNA encoding insulin-like gland hormone from *Scylla paramamosain*, named *Sp-IAG*, was identified. The predicted protein had similar molecular organization to other insulin-like androgenic gland factors reported in the Decapoda, encoding a signal peptide, B chain, C peptide and A chain. There were two disulfide bridges between the B chain and A chain, and one disulfide in the B chain. In particular, a full genomic DNA sequence of *Sp-IAG* with a 5′ flanking region of 2988 bp was revealed from which many potential regulatory binding sites were first identified in *S. paramamosain*. The *Sp-IAG* gene was highly expressed in the androgenic gland and also lowly expressed in the seminal vesicle and ejaculatory duct, which was not reported in previous studies. It is noteworthy that Sp-IAG was highly expressed both in the androgenic gland and in the seminal vesicle using western blot analysis, suggesting that Sp-IAG might play a major role in these two organs. In addition, it was quantitatively detected that *Sp-IAG* mRNA expression was up-regulated after mating, which suggested that this protein might have an activity related to mating behavior. Eyestalk ablation can induce a high level of *Sp-IAG* expression, demonstrating that the *Sp-IAG* of *S. paramamosain* was negatively controlled by the X-organ–sinus gland in the eyestalk. These findings provided the basis for elucidating the mechanism of sex differentiation in crustaceans.

1. Introduction

Scylla paramamosain is an important marine aquaculture species, which is distributed in the IndoWest Pacific region. Mature female crabs have a relatively high market value because of the rich yolk in the gonad which is known to be nutritious. Crustacean breeding is now prone to be monosexual for commercial purposes. Monosex aquaculture is now acknowledged and has been widely used in fish farming (Hunter et al., 1983; Jensen and Shelton, 1979). Hormonal induction of sex reversal is the most widely used technique available to mass-produce monosex populations of fishes (Singh, 2012). However, due to the fact that the regulation mechanism of crustacean sexual determination and differentiation is still ambiguous, reports on crustacean monosex breeding are rare. In recent years, study of the androgenic gland (AG) hormone gene has increased the possibility of manual sex control, thus bringing huge commercial interests to aquaculture (Ventura and Sagi, 2012). The latest research on *Macrobrachium rosenbergii* obtained the sex-reversed female by silencing the AGH gene (Panigrahi et al., 2012). Because of this, understanding more concerning IAG will be of great significance in terms of reasonable application in aquaculture in the future.

The AG was first found in *Callinectes sapidus* in 1947 (Cronin, 1947). Charniaux-Cotton (1954) later identified the AG, and suggested that it was involved in sexual differentiation and spermatogenesis. Following this, more work on elucidating the role of the AG in isopods and decapods was carried out, particularly in the Decapoda. Charniaux-Cotton (1954) first successfully removed the AG of male amphipods and implanted it into females. Since then, multiple analogous studies have been conducted, and those experiments revealed that AG-implanted females were masculinized and AG-ablated males feminized (Barki et al., 2006; Katakura, 1960; Khalaila et al., 2001; Malecha et al., 1992; Manor et al., 2004; Nagamine and Knight, 1987; Nagamine et al., 1980; Puckett, 1964; Sagi et al., 1990; Suzuki and Yamasaki, 1997; Taketomi and Nishikawa, 1996). Most AGs are found alongside the distal area of the male ejaculatory ducts (ED), and act via a hormone secretion. These findings support that the AG plays a vital role in male sex differentiation, and maintains individual primary and secondary sex characteristics. They also suggest that AG is associated with spermatogenesis in

* Corresponding author at: Center for Marine Biotechnology, College of Ocean and Earth Sciences, Xiamen University, Xiamen 361102, PR China. Tel.: +86 592 2184658; fax: +86 592 2180655.
E-mail address: wkjian@xmu.edu.cn (K. Wang).
[1] Both authors contributed equally to the article and both should be considered as first authors.

http://dx.doi.org/10.1016/j.aquaculture.2014.06.033
0044-8486/

crustaceans. This provided some clues for further elucidating the mechanisms of sex determination and differentiation in crustaceans.

It is known that some congenital factors contribute to sex development in crustaceans, including the gonad inhibitory hormone produced in the X-organ–sinus gland (XO–SG) and gonad stimulating hormone in the brain and thoracic ganglion. Both of these hormones are important reproductive regulators (Eastman-Reks and Fingerman, 1984; Ōtsu, 1963). In a few decapods, eyestalk ablation (ESA) leads to hyperplasia of the AG (Chung et al., 2011; Hoffman, 1968), implying that XO–SG is the negative regulator of AG. This is described as the eyestalk–AG–testis endocrine axis, which shows direct inhibition by XO–SG on the AG (Khalaila et al., 2002). However, whether there was also eyestalk–AG–testis axis existed in *S. paramamosain* has not yet been confirmed, much less is known about the reproductive physiology of male *S. paramamosain* at the molecular level.

The first cDNA of the molecular AG hormone (AGH) was cloned from the AG in the isopod *Armadillidium vulgare* (Okuno et al., 1999). At present, several insulin-like AG-specific genes in the Decapoda have been identified, most by construction of an AG cDNA subtractive library (Manor et al., 2007; Sroyraya et al., 2010; Ventura et al., 2009). More recently, an insulin-like AG factor (IAG), *Cas-IAG*, was identified using degenerate PCR (Chung et al., 2011). Two spliced variants of insulin-like AGH gene in *Fenneropenaeus chinensis* were identified, and this is the first report of two distinct variants of IAG transcripts in crustaceans (Li et al., 2012). A newly found AG-specific gene, *Mn-IAG*, is also isolated from a transcriptome library of *Macrobrachium nipponense* (Ma et al., 2013).

In this study, we employed degenerate PCR to identify a novel insulin-like AG-specific gene *Sp-IAG* (GenBank accession no. JQ681748), in the mud crab *S. paramamosain*. The genomic sequence and promoter region were obtained using a genome walking approach, which first revealed the full genomic DNA sequence and many potential regulatory binding sites were identified. Tissue-specific expressed *Sp-IAG* mRNA transcripts implied its importance in gender determination. Also, western blot

A

Sp-IAG (JQ681748)

```
1     gcggtgcatcatcaggagctgctcttggcacttgacacctcggcacggcacggcacggca      60
61    caccttccgcccgccacgcccttccgccacctcttccttttctagtcagcagcaactact     120
121   tctcctggcctgtactacgttttctttggcctcccttccagcctgcattcaattcgccct     180
181   tgtctggtttgcctcctccagcttgggtcctccacataactttcagcccgtgtacgccac     240
241   cgccaagaATGTGTCCGCGTGTGATCTTAATCCTGGTGCTGCTGACGGCGACGCAGACG      300
1                M  C  P  R  V  I  L  I  L  V  L  L  T  A  T  Q  T      17
301   AAGGCGGATCTTATTAGCGACTTCTCCGTGGACTGTGGTAACCTACTGAGATCCTTTTCC     360
18    K  A  D  L  I  S  D  F  S  V  D  C  G  N  L  L  R  S  F  S      37
361   TCCGTTTGCCTCACCTATAAACAACCTCTCAGCGAAAGATATAAACGAGGCACAGAAACA     420
38    S  V  C  L  T  Y  K  Q  P  L  S  E  R  Y  K  R  G  T  E  T      57
421   AAGGGCGCGGCTTCCTTTGACGATGCTACCACTGAATTCCGTCCCCGTCCGCTTCACGTT     480
58    K  G  A  A  S  F  D  D  A  T  T  E  F  R  P  R  P  L  H  V      77
481   CTCCTCGCGGAACAAGACGAAGACCCGATGCTGCCCCCAGAAGACGCCTTCCAACTCGTC     540
78    L  L  A  E  Q  D  E  D  P  M  L  P  P  E  D  A  F  Q  L  V      97
541   AAGACTCATTGGACAAGAGAAAGGTTCCGCAGGTCCCACCGGGACGTGAATGGCTATGAC     600
98    K  T  H  W  T  R  E  R  F  R  R  S  H  R  D  V  N  G  Y  D     117
601   GAGTGCTGCCCGCAGTCCACCAAGAACTGCACTGTGTATGAGGTGGCCGAGTACTGTAAC     660
118   E  C  C  P  Q  S  T  K  N  C  T  V  Y  E  V  A  E  Y  C  N     137
661   AGCCTCAGGCCCCCGTATAGGGAACTCTTAGCTTCCAGAAAGAGGCAGTAAaagtaggagg     720
138   S  L  R  P  P  Y  R  E  L  L  A  S  R  K  R  Q  *               153
721   aggacaacgcggccactgctgctccgaacaatttaagtcagttcacttcgcagtctcgtc     780
781   attttcgtccgtatcttccttccaaatgaggtactaaaggaatatgtttacaaaattatc     840
841   acttcacatccttacaatttttttttttttcggtacgggttagaaaaggtaaaagtaat     900
901   tgcaaaacctgaaaatttccatccgtctcctccctctagaaggcactattgaaggatttg     960
961   tgtttgcagaattcttacctcacgcctccacttgtttcatctttccaaaaacaccagagg    1020
1021  aagatcaacatcaagatcaacaagttatcgcttcagaacctgacaattttcattccatgc    1080
1081  ggtctaaaaaagttcgtaaaagttcatgctaacaaattaaagcttcataacctaataatt    1140
1141  ttgcatcccttccatgcccctccccactcataaaaaaaaaaaaaaaactaaactaacattt    1200
1201  ttaacaaatcaataatttgcaaactgaaactgttcatccattccaatctctctttcaca     1260
1261  aaaaaaaaaaaaaaaaaaaaaaaaaaaaa                                   1290
```

Fig. 1. A. Sequences of the full-length cDNA and deduced amino acids of Sp-IAG. The start of the ORF (ATG) is shown in bold, and a stop codon (TAA) is shown in bold and marked with an '*'. The predicted signal peptide is shown in bold italics. The amino acid sequence of the C peptide is flanked between the B and A chains and is underlined in bold. The predicted cleavage sites are marked with squares. A putative N-linked glycosylated site is shaded. B. A sketch map of B and A chains of disulfide bridges in Sp-IAG. C. Neighbor-joining phylogenetic tree of Sp-IAG amino acid sequences from different species. One thousand bootstrap trials were run using the neighbor-joining algorithm using the MEGA 5.0 software. The species and their GenBank accession numbers are given in Supplementary Figure S1. D. The structure of *Scylla paramamosain Sp-IAG* genomic DNA and cDNA. Exons are indicated by boxes and introns are indicated. Length of the introns and exons are labeled on the diagram and expressed in terms of base pairs. E. Deduced promoter region of the *Sp-IAG* 5′ flanking sequence. Putative HSF, Sox-5, cap, C/EBPb, ER, GR, and PR binding sites are underlined. Putative Skn-1, GATA-1, Dl, GC-box, NKx-2, and GATA-3 binding sites are shaded. Putative CREB, ADR-1, Dfd, Hb, GATA-2, PBx-1, and MZF1 binding sites are in bold. Putative SRY, CRE-BP, P300, AML-1, AP4, NIT2, and CdxA binding sites are indicated with an arrow.

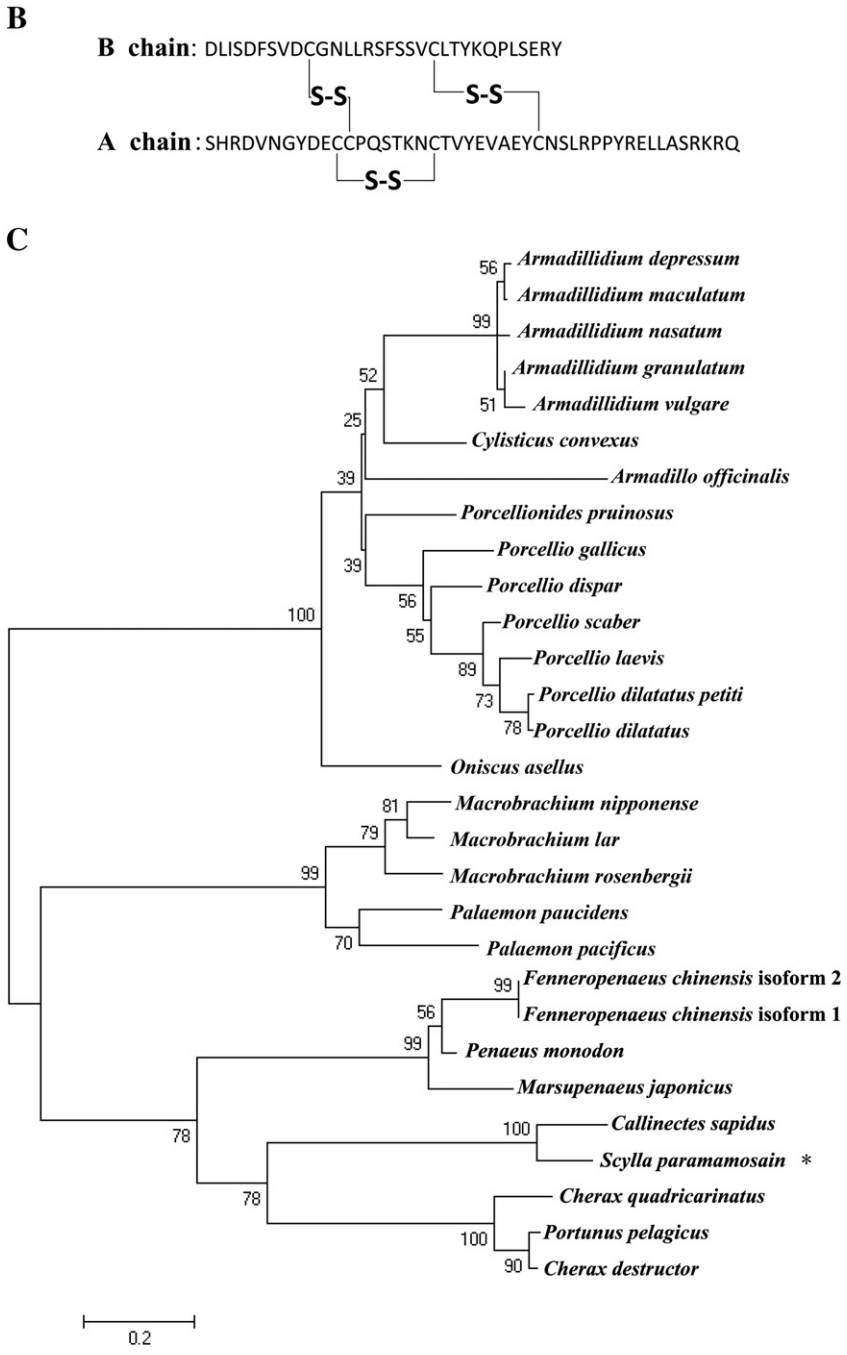

Fig. 1 (*continued*).

detected Sp-IAG in the AG and seminal vesicle (SV). The *Sp-IAG* level was elevated in the mating season, and it was up-regulated by ESA in both the AG and ED, which confirmed an eyestalk–AG–testis axis existed in *S. paramamosain*.

2. Materials and methods

2.1. Animal and tissue collection

Live healthy mud crabs (*S. paramamosain*) purchased from local breeding farms close to Xiamen, China and were maintained at an aquatic breeding farm of Xiamen University under the following conditions: Animals were fed sea clams once per day, and sea water was purified through a bio-filter and renewed daily to ensure water quality. Hemolymph samples were immediately subjected to centrifugation at 800 *g*, at 4 °C for 10 min to collect hemocytes. Other tissues including the thoracic ganglion, midgut, brain, gills, heart, hepatopancreas, stomach, testis, SV, ED and AG, together with parts of the posterior ejaculatory duct (PED) as well as the penis, muscle and eyestalk were surgically obtained and immediately frozen in liquid nitrogen. The AG was collected with the PED, because it is fragile. There were five replicates for each tissue. Samples were stored at −80 °C until use.

2.2. Nucleic acid preparation

The total RNA from different tissues was extracted using Trizol Reagent (Invitrogen), quantified with a NanoDrop spectrometer (Thermo Scientific), and then treated with RQ1 RNase-free DNase (Promega, USA)

D

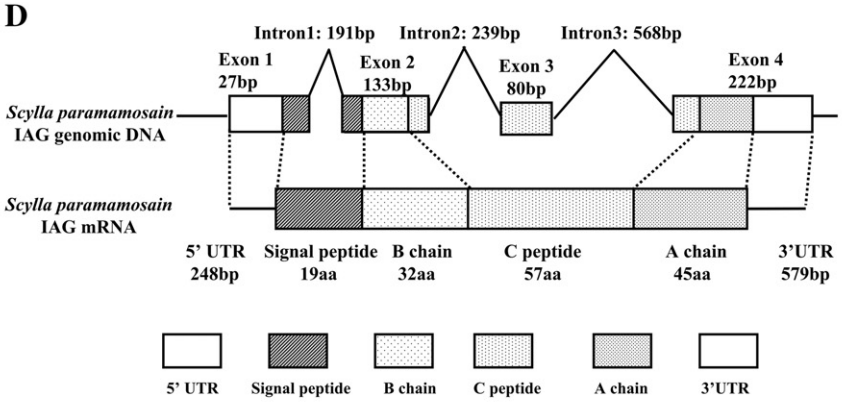

E

```
-2988 TCCTCGTATCTCGACTGCGTGAACAGGTTCTATTGGAAATTATTTCAGGTTTTCAATGGT
                NIT2/ GATA-1          HSF
-2928 GGTTTCATGATTCTGGTAATAGTTTAAGAAGGATTTCACGTAATAGAAAAAAAAAACTCT
          Skn-1/HSF/Dfd          HSF      CRE-BP      Hb
-2868 TCCCCTTTACCTCTTGTACGTCGCTTTTCTCTTCCCCTCCCTTCCCTTCCTTTCTCCTC
                                  DI      ADR1     MZF1     HSF
-2808 TTTTTCCATCATTTCCTTCCTTTCCTTCCTTTTCTCCGAGCCTCCAGCTCTTAGGATGCG
            Cap                                ADR1
-2748 TCCACACGGTCGAACACTGTCTGACAAACACTGTTACCGTATCATAAGACGAAGCAGGAT
                GR
-2688 GACGTCATACTACGGACACGGGCAGTGTCCACTAGACCTTTTGGTGCTCGCTGGTGACGT
      CREB/CRE-BP/cap          cap                    CREB/CRE-BP
-2628 CATTGACGCTCCTTTCCGCTTCCCATTGTTAACTGGTAACAGCGGGTGTTCGACGGACAA
            SOX-5/CREB/SRY          AP-4
-2568 TGTTCGACAGTGTGGACACGCCCTTGACTATCTTGCTCAAACATTTGCCACCACCAGTTG
                GATA-2/NIT-2/C/EBPa
-2508 TCTCTGTGCACACGACAAGCCCTCCACATCATCCTGTTTTTAACCTGTGCCGTCTTGATA
                ADR-1/GATA-1/cap          ER        NIT-2
-2448 TTACAGGCCATTCGTACGAGTAAGTTCGTATTCTCCAACATTTCGGCGTCTTATTTCGGT
-2368 TACTTTTAACAATCAAGATATTAGGGTATTTGCGGACGCTTTCATGATTCTAGCGGCGGA
            Sox-5/PBX-1 /NIT2          Skn-1/HSF
-2308 CTGTCTTCTGCCGATCTCTCTCTTCGCCGCAGGGTTGTGTGTCTGGCTATCTTCTAGTAA
            HSF                                GATA-2/ NIT2
-2248 GATTTCTTTCACGCTAATTGTTCTTCTGGTCTTACTAACTTCATGCCTCCTTCACTCCCG
            HSF/SRY          Sox-5                  ADR-1/p300/cap
-2188 CTTCCTCACTACACAAGGCTTTCTACATTTTCTGATCCCTATTTTGTTCACCTCCATAAT
                                    HSF          cap/ADR-1
-2128 GCAAGAGTTTTTTTCATTTCTTCTGCTGAGAAACTCTGGAATTCTCTGTTTCTGTATTTC
                  cap/HSF                SRY
-2068 TTTTTACCTTTGACTTGAACTGTTTCAAGGGAGAGGTTGCAACACATTTCTCTAGTTTTG
            SRY                    C/EBPb          SRY
-2008 AGTAATCTTTCGTTGATCTGTACTCTACTTGGACTGGCGCCTTCGGTAGCCCCTCCCCCT
            C/EBPa                    cap              GC box/ADR-1
-1948 CCCTTTTTTTTTAATATAACTTTTTTGTTGGCCGCAGCCAGAACCAATCTTACGTAAAAA
                  CdxA          Hb                    CRE-BP/Hb
-1888 AGTTTAACCAAGATTCTGTACCATCAATGGAAGAAGCACTCATGATACTCACAAGTCAAT
                  HSF          CdxA          Skn-1/NIT-2  ER
-1828 CACCTCTGTTGTCTCTGAAGGTAGTCTGTCTAAGAGTCTGAAGTGATGAACACGGGCCGT
                                          cap/Nkx-2/cap
-1788 ACAGACAAGGTCAATGGTCACAGCAACAAAGAGTAACAGTTACACTTACTTTCACTGTAT
                  COUP-T                          Nkx-2
-1728 TCAGCGTTCTCCCTCAGTCTTCAATAACCTGAAATGCTAAAAATCTATCAGTAATATATT
            cap  HSF          cap                        Dfd/CdxA
-1668 CTATAAAGAGATTATCACTCAGCCGAATACAGGTATTGTTAACCTAACCTAGCTTAACCT
            HSF          NIT-2          SRY/SOX-5
-1608 AATGTATCTAACCTATTTTGTAAGAACATTGTCATTCAGCAGATTAGTCTAAAATTAAGG
                  NIT-2          PR      Skn-1/cap          Nkx-2
-1548 GAAGAAGACGAACACAGTGGAAGGGAGTGTAGGCTAATCGACTTCGCTCAGTGTACACAG
                  GR          P300/ADR1                cap

-1488 GCGTATGACCCGAAACATACGGAATGGTTGCCAACTTGTTATATTTTCAGTTAGTTTGAA
            cap          HSF/SRY                    CdxA
-1428 TAGAAAACATGGCGTTGTTTTGTAAATACTGTATAGGGAGTGTGTGTGTGTGTGTGTG
            HSP                SRY          ADR-1/P300
-1368 TAAGGCGTCATAGAAAAGCTCATTGAAGTGTACAAACAAAAACAAATAAAGCGTGTATTC
                        CdxA          Nkx-2  GR  SRY
-1308 TGTGGTAAATAAAAGTTTTCGTTTCGTTTTGAAATAATATCTTTCCCACTCAGCAATGCG
      CEBP/AML-1A                SRY
-1228 ACCATATTGCCAACACACACACACACACACACACACACACATCATTTATCACAACAAT
                  C/EBPa                              CdxA/NIT2
-1168 CAAGCGCTACAAGTCACTAATTAACTGTTACACCCTCGCTGGCTTTATCAACCACATTGC
                                                      AML-1A
-1128 CGATAGTGTTTCCTGACCACCGAGCACTGGACAGGAATGCACCGTTCTTCCCCTTGACAC
      GATA-1                          cap          ADR-1
-1068 CCTCTCATTGTTCCTGCCTCGTCATATCGCTCCCCTCTTCTCCAACGACCTCGCTTCTCG
            Cap/HSF          NIT2      MZF1
-1008 TATTTCTGTCGTACGGCGCCATATGACCTTGCTGATGCGGCGCAACTCACCTCAGTCAAA
            CdxA/HSF                GATA-1/GATA-2          cap/SRY
-948  CAAAGGTAATTTTCTTGCACTCTAAGTAAAAATTAGCAAAACAGACGAAAATATCAAAAC
                  Dfd
-888  GCCAAACACACGTAAAAGATAAAAAGATGTAGATCGAATTGTTACTAAAATAATTCTTTC
            SRY          GATA-1/NIT2          Sox-5    CdxA/Dfd
-828  TCACTATCGTTCTTTATAGTACGAAGAAAGAGAAAGGAAAGGAGGAGGGAAAGAAAGGAAAGG
            cap/GATA-3/HSF/CdxA          HSF          ADR-1      HSF
-768  GAAGGGTAGAGAAACATGACAGGAAAGAAGAAAAAAGGAGGTAATGAAAGGGAAGAAAGA
                        HSF                Hb          Dfd/cap
-708  AGAAAAGGAAAGAGAAGAAAAGGAAGGGAAGGGAGGGGAAGAGAAAAGCGACGTACAAGA
            HSF          HSF                MZF1      DI
-648  GGTAAAGGGGAAGAGTTTTTTTTTTCTATTACGTGAAATCCTTCTTAAACTATTACCAGA
                                    CRE-BP          Dfd
-588  ATCATGAAACCACCATTGAAAACCTGAAATAATTTCCAATAGAACCTGTTCACGCAGTCG
      Skn1
-528  AGATACGAGGAAACCGCTGAAACTTGTCAACATGCGGAGATTAAGGCTGAGACAAAACAC
      GATA-1/NIT-2          CAP                ADR-1      cap      SRY
-468  AAAATAGAAAAGTAGAGGTGTTAATCAAGCCCTGACCGAGCACACTGCTGTCACTGAGGG
                  HSF          Dfd/CdxA    ER
-408  GAGGGCGAAGAGCAACAATCAGCACCTTAAAACAATTGCTGCTTGAACGGAGACGTCACA
      ADR-1                          Sox-5                CREB
-348  ATGTCAAAACAAGTCAAGGTTCTGAGCATACAATGGCCTCTTGGTGGTTATGGTGCCAAC
                        HSP    cap
-288  ACTCTGGGTATATAAGCTTACACATGGAGCTCCTTGGCCTGCGGTGCATCATCAGGAGCT
                              ADR-1          TSS
-228  GCTCTTGGCACTTGACACCTCGGCACGGCACGGCACGGCACACCTTCCGCCCGCCACGCC
-168  CTTCCGCCACCTCTTCCTTTTCTAGTCAGCAGCAACTACTTCTCCTGGCCTGTACTACGT
-108  TTTCTTTGGCCTCCCTTCCAGCCTGCATTCAATTCGCCCTTGTCTGGTTTGCCTCCTCCA
 -48  GCTTGGGTCCTCCACATAACTTTCAGCCCGTGTACGCCACCGCCAAGAATG
                                                      -1
```

Fig. 1 (*continued*).

to remove the contaminated DNA. The RNA quality was assessed using electrophoresis on a 1.2% agarose gel. The cDNAs for spatial and inducible expression profile analysis were synthesized from 1 μg total RNA with a PrimeScript RT-PCR Kit (TaKaRa, Japan) following the manufacturer's protocol. The 5′ RACE and 3′ RACE cDNA were prepared with a SMART RACE cDNA Amplification Kit (Clontech, USA) following the manufacturer's protocol and were used as a template for PCR. The genomic DNA was purified from a muscle using a Universal Genomic DNA Extraction Kit (TaKaRa, Japan). The genomic sequence and promoter region were obtained using a genome walking approach with a GenomeWalking Kit (TaKaRa, Japan).

2.3. PCR with degenerate primers

The degenerate primers listed in Fig. 1 were designed based on the conserved amino acids found from the multiple alignment ClustalW (http://www.ebi.ac.uk/Tools/clustalw2/index.html) of deduced amino acid sequences of IAGs of *Cherax quadricarinatus* (GenBank accession no. DQ851163), *M. rosenbergii* (FJ409645), *Penaeus monodon* (GU208677), *Portunus pelagicus* (HM459854) and *C. sapidus* (HM594945). PCR conditions were as follows: 94 °C for 5 min; 35 cycles at 94 °C for 45 s, 45 °C for 45 s, 72 °C for 1 min and the final extension at 72 °C for 7 min. The PCR products were analyzed on a 1.5% agarose gel. Expected PCR products were purified from the gel using a Qiaquick Gel Extraction Kit (Qiagen), and ligated into the vector pMD18-T (TaKaRa) followed by transformation into *Escherichia coli*. The positive clones identified using PCR were sequenced at least twice at Shanghai Sangon Biological Engineering Technology & Services Co., Ltd. (China).

2.4. 5′ and 3′ RACE of Sp-IAG

The PCR produced by the generate primers was blasted using the BLAST program (http://blast.ncbi.nlm.nih.gov/Blast.cgi), and it had a close affinity to *Cas-IAG* (GenBank accession no. HM594945). Two specific primers, listed in Table 1, based on *Cas-IAG* were designed to obtain the larger fragment. The PCR product was cloned and sequenced as before. *Sp-IAG*-F1, *Sp-IAG*-F2, *Sp-IAG*-R1 and *Sp-IAG*-R2 (Table 1) were designed based on the fragment obtained from homology-based cloning. The 5′ end and 3′ end of the *Sp-IAG* were cloned using nested PCR with a RACE template from the AG together with parts of the PED. The 3′ end of *Sp-IAG* was cloned using primer *Sp-IAG*-F1 and 3′ CDs primer in the first round PCR and *Sp-IAG*-F2 and 3′ CDs primer in the second round PCR. The 5′ end of *Sp-IAG* was cloned using primers *Sp-IAG*-R1 and the 5′ CDs primer in the first round PCR and *Sp-IAG*-R2 and the 5′ CDs primer in the second round PCR. All the PCR products were sequenced following the procedures described above.

2.5. Cloning of the genomic DNA and the promoter of Sp-IAG

The genomic sequence and promoter region were obtained using a genome walking approach with Genome Walking Kit (TaKaRa, Japan). Three gene-specific primers (GSPs) based on known sequences of 5′ UTR of *Sp-IAG* and four shorter degenerate AP primers from the kit were used for genome walking. Primers for introns (*Sp-IAG*-F3 and *Sp-IAG*-R3) were produced based on the obtained sequences of *Sp-IAG*. All primers used for amplifying the introns and the promoter region are listed in Table 1. Sequences of the four AP primers from the kit were unknown. Reaction volumes and amplification cycling conditions were following the manufacturer's instructions. Specific PCR products were cloned and sequenced as before.

2.6. Sequence analysis

AGH and IAG sequences from different organisms were obtained through the NCBI BLAST search program. A multiple sequence alignment was created by ClustalW. Phylogenetic relationship of the IAGs and AGHs was analyzed using the neighbor-joining method, and the reliability of the branching was tested using bootstrap resampling (with 1000 pseudo-replicates). Fig. 1c was drawn using the MEGA 5.0 software. Sequences of the 5′ flanking region were analyzed with TRANSFAC and AliBaba 2.1 software (http://www.gene-regulation) for potential transcriptional factor binding sites.

2.7. Quantitative analysis of Sp-IAG expression

Tissues of five healthy crabs (about 300 ± 20 g in weight per crab) including hemocytes, thoracic ganglion, brain, gills, heart, hepatopancreas, stomach, midgut, gonad (testis, seminal vesicles, ED, AG and penis), muscle and eyestalks were obtained for total RNAs. Total RNA extraction was performed using Trizol Reagent (Invitrogen), and treated with RQ1 RNase-free DNase (Promega, USA) to remove the contaminated DNA. RNA integrity was electrophoretically verified by ethidium bromide staining and by OD260/OD280 nm absorption ratio >1.95. A mass of 1 μg of total RNA for each tissue was separately reverse-transcribed in a final volume of 20 μL using a PrimeScript RT reagent kit (Perfect Real Time) (TaKaRa) following the manufacturer's instructions. *Sp-IAG*-QF and *Sp-IAG*-QR (Table 1) were used as forward and reverse primers. Real-time PCR was performed in a reaction mixture of 20 μL containing 1 μL of total transcribed cDNA, 6 pmol of each primer and 10 μL of Power SYBR Green PCR Master Mix (Applied Biosystems, UK). The standard cycling conditions were 95 °C for 10 min, followed by 40 cycles of 95 °C for 15 s and 60 °C for 1 min. Data of raw relative quantification were calculated using 7500 system SDS software version 1.3.1.21 and the *β-actin* gene was employed as the internal standard, and processed using SPSS 16.0. Melting curve and standard curve analyses were carried out for specificity and efficiency of the primers.

2.8. Eyestalk ablation

Mature males (about 150 ± 20 g in weight per crab) were randomly divided into two groups: (1) a control (no ESA), and (2) a bilateral eyestalk-ablated group. Two eyes from each experimental male were cutoff using aseptic techniques. The two groups of crabs (including controls) were reared in a rectangular tank independently. At days 0, 3, and 7, following the ESA, five crabs from each group were sacrificed and the AG from these crabs were collected and prepared for total RNA. The expression level of *Sp-IAG* was determined using qRT-PCR analysis as described above. Each sample (20 ng of total RNA equivalent of cDNA) was assayed in triplicate using SYBR Green (Applied Biosystems) with the primers: *Sp-IAG*-QF and *Sp-IAG*-QR (Table 1). The result was studied using 7500 software 2.0.1, and processed with SPSS 16.0.

2.9. Preparation of polyclonal antibody against Sp-IAG

The recombinant protein pET28-Sp-IAG was expressed in *E. coli* induced by IPTG for antibody preparation. Five mice were used to produce a polyclonal antibody against the Sp-IAG peptide. For the first immunization at day 0, 200 ng of the recombinant protein pET28-Sp-IAG was mixed with a 1.5 mL volume of complete Freund's adjuvant, and injected subcutaneously into every mouse using aseptic techniques. For the first to third boosts, at weeks 2, 3 and 4, 150 ng of the protein pET28-Sp-IAG was mixed with a similar volume of the incomplete Freund's adjuvant, and then injected using the same protocol. Pre-immune serum was collected from each mouse before the first immunization. The blood was collected at one week after the final boost, centrifuged at 5000 *g* for 15 min, after which the antiserum was collected and stored at −80 °C until use.

2.10. Immunofluorescence staining

The PED of adult crabs were carefully removed and stored at −80 °C until ready for sectioning. Then the tissue sections were fixed with 4%

Table 1
'D' represents degenerate primers, GSP represents gene-specific primers for 5′ flanking sequences, and GM stands for primers for genomic sequences. QF and QR stand for primers for real-time PCR.

	Primer sequences
DF	GAYTTYGAYTGYGGNSAYYT
DR	RCARCAYTCRTCRTANACRTT
GSP1	ACGGGCTGAAAGTTATGTGGAGGACC
GSP2	GGCCAGGAGAAGTAGTTGCTGCTGACT
GSP3	GTGCCGAGGTGTCAAGTGCCAAGAG
Sp-IAG-F1	CTGACGGCGACGCAGACGAAGG
Sp-IAG-F2	TTTTCCTCCGTTTGCCTCACCTAT
Sp-IAG-R1	CTGACTATTTCGGGAAGCAAGGAG
Sp-IAG-R2	ATCCTTTTCCTCCGTTTGCCTCAC
Sp-IAG-F3	TCCGCGTGATCTTAATCCTGGTGCTG
Sp-IAG-R3	CTGACTATTTCGGGAAGCAAGGAGTTCC
Cas-IAG-F	GTGACGGCAACGCAGACTAAGG
Cas-IAG-R	CTGACTATTTCGGGAAGCAAGGAG
Sp-IAG-QF	TAAACGAGGCACAGAAACAAAGGGC
Sp-IAG-QR	AACCTTCCTCTTGTCCAATGAGTCTT
β-Actin-F	GCCCTTCCTCACGCTATCCT
β-Actin-R	GCGGCAG TGGTCATCTCCT

formaldehyde (pre-cooled acetone), and the slides were rinsed in 200 mL of 10 mM phosphate buffered saline (PBS) pH = 7.4. The slides were incubated in 3% H_2O_2 solution in methanol at room temperature for 20 min. This step was to block endogenous peroxidase activity. Then the slides were rinsed in 200 mL PBS for two changes, 5 min each. The sections of the slides were blocked with non-immune serum and incubated in a humidified chamber at 37 °C for 30 min, and then incubated with anti-Sp-IAG polyclonal antibodies or negative serum (1:100 dilution in PBS) for 1.5 h at 37 °C in a humidified chamber. After washing three times with PBS, the sections were incubated with a FITC-conjugated goat antimouse IgG secondary antibody (1:100 dilution in PBS) (Antigenix) at 37 °C for 1 h. Then the slides were washed again, and the sections on the slides were incubated with an appropriately diluted DAPI solution (0.25 μg/mL) at room temperature 15 min. Finally, after washing twice in PBS, the sections were mounted with coverslips using mounting medium. The color of the antibody staining in the tissue sections was observed under a Leica fluorescence microscopy imaging system.

2.11. Western blot

Tissue samples were dissolved in RIPA buffer and homogenized using an electric homogenizer (IKA, Asia). After centrifugation at 12,000 *g* at 4 °C, the protein concentration in the clear supernatant was determined using the Bradford method. Protein samples were separated using Tris–glycine SDS-PAGE (15%) and transferred onto PVDF membranes. The membrane was blocked for 1 h at room temperature with PBS supplemented with 0.1% Tween-20 and 5% nonfat milk and then incubated for 1.5 h at 37 °C with anti-Sp-IAG polyclonal antibody (1:500). β-Actin antibody (Santa Cruz Biotechnology) was used as internal reference to certify the integrity. After washing four times with PBS containing Tween-20, incubated with HRP-conjugated goat anti-mouse secondary antibodies (1:5000 dilution) at 37 °C for 1 h. After washing, chemiluminescence substrates (ECL, Millipore) were used to reveal positive bands, and bands were visualized after exposure to Hyperfilm ECL.

3. Results

3.1. Molecular characterization of cDNA, genomic organization and amino acids predicted

The full-length cDNA (1289 bp) of *Sp-IAG* (GenBank accession no. JQ681748) was isolated from the AG together with parts of the PED using PCR, followed by 5′ and 3′ RACE. The *Sp-IAG* consisted of a putative coding region (462 bp) and had flanking regions with a short 5′ UTR (248 bp) and a long 3′ UTR (579 bp). The open reading frame (ORF) of *Sp-IAG* cDNA was predicted using DNAssist 2.0 software. The deduced protein of *Sp-IAG* cDNA was 153 aa with a predicted mass of 18 kDa. The first N-terminal 19 aa was predicted to be a signal peptide using the SignalP 4.0 Server (http://www.cbs.dtu.dk/services/SignalP/). Sp-IAG had structural homology with the insulin-like family proteins: a signal peptide in its N terminus (19 aa), six cysteine residues aligned with AGHs and IAGs, and B and A chains (32 and 45 aa, respectively) separated by a C peptide (57 aa) with two putative cleavage sites predicted, RYKR and RFRR, joined to the B and A chains, respectively (Fig. 1A). The B and A chains of Sp-IAG were configured by two putative interchain disulfide bridges formed between the Cys residues located in the B chain and those located in the A chain, respectively. Two Cys residues located in the A chain formed an intrachain disulfide bridge (Fig. 1B). Moreover, a putative N-linked glycosylated site was found in the A chain.

The *Sp-IAG* genomic DNA consisted of about 2287 bp (GenBank accession no. JQ681745) and contained four exons and three introns (Fig. 1D). All exon–intron junctions followed the consensus rule of the splice acceptor – AG/GT – splice donor for splicing.

3.2. Multiple sequence alignment and phylogenetic analysis of Sp-IAG

Multiple sequence alignment of Sp-IAG with other known IAGs or AGHs is shown in Supplementary Figure S1. It had an outstandingly high similarity (81.7%, calculated with DNAMAN Version 6.0) with *C. sapidus*, but it shared very low identities with other IAGs and AGHs (16.45–24.86%), among which six cysteine residues were conserved in all crustacean species: two cysteines in the B chain (marked by an asterisk), and four cysteine residues in the A chain (marked by an asterisk). In the Isopoda, there were another two conserved cysteine residues (boxed in red) in comparison with the Decapoda. A neighbor-joining tree of *Sp-IAG* amino acid sequences was constructed based on the amino acid sequences of AGHs and IAGs using the neighbor-joining method (Fig. 1C), and the phylogenetic tree showed far evolutionary distance between the Isopoda and the Decapoda. Furthermore, the IAGs of the Decapoda were divided into three groups, the Palaemonidae, Penaeidae, and Parastacidae and Portunidae (Fig. 1C).

3.3. Analysis of promoter sequences of Sp-IAG

TRANSFAC and AliBaba 2.1 software (http://www.gene-regulation) analyses of the sequence upstream of the transcription start site revealed a number of putative transcription factor binding sites, including ICSBP, Oct-1, Sp1, TBP, C/EBPbeta, C/EBPalp, NF-1, NF-kB, GATA-1, AP-1, HSE, YY1 and SRY (Fig. 1E).

3.4. Androgenic gland-specific expression of Sp-IAG in male S. paramamosain

Quantitative analysis revealed that *Sp-IAG* was expressed specifically in the AG including parts of the PED in male *S. paramamosain* (Fig. 2A). We ruled out the confusion caused by PED using another PCR in which *Sp-IAG* was not expressed in the AG-ablated PED. However, the SV and ED also had a low level of *Sp-IAG* expression. Examination of *Sp-IAG* in the female crab using RT-PCR revealed that it was not present in any of the tissues (Fig. 2B). Genomic DNA contamination was ruled out since *Sp-IAG*-QF and *Sp-IAG*-QR were designed over an intron. Results from western blot showed that Sp-IAG was found in both the AG and SV (Fig. 2C).

3.5. Immunofluorescence for Sp-IAG

Specific green staining was clearly observed and distributed in the AG which attached to the posterior ejaculatory duct, and which could be observed more clearly using a higher magnification. However, in

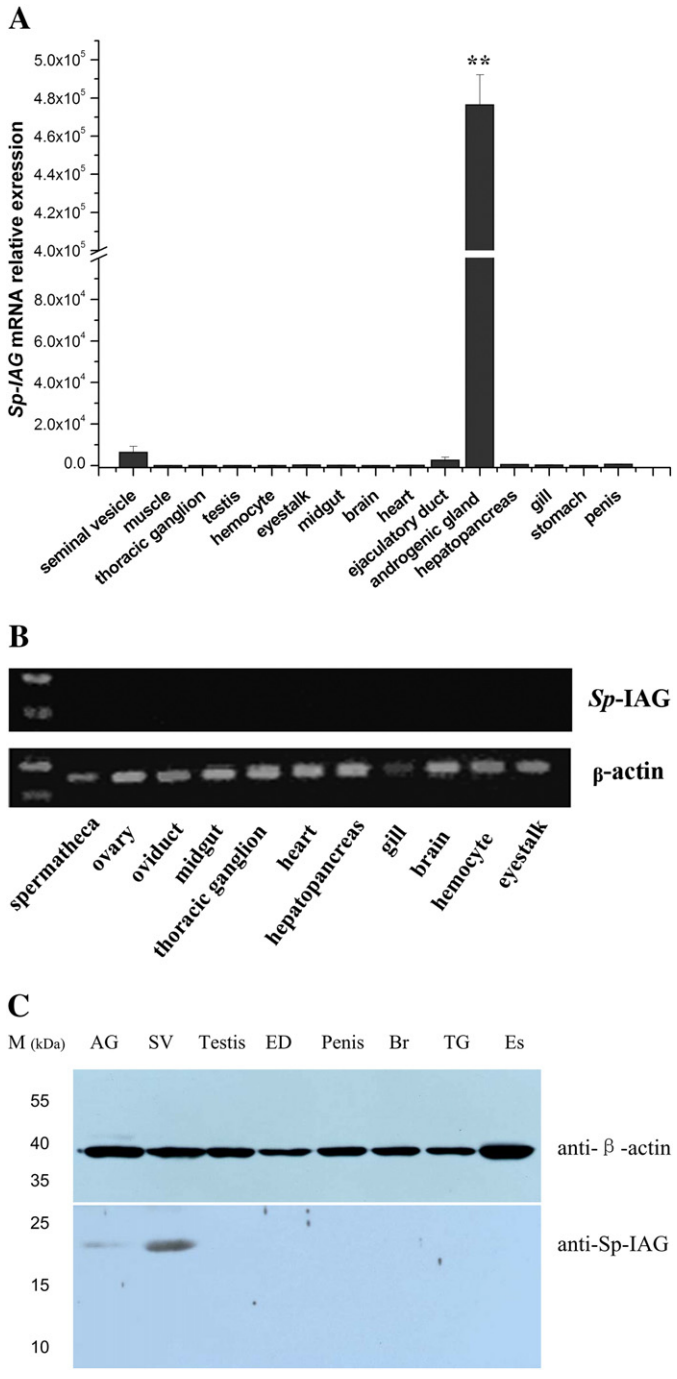

Fig. 2. A. Relative gene expression of *Sp-IAG* in different tissues of male crabs detected using real-time PCR. The data presented includes the mean and standard errors of the mean derived from triplicate experiments (*$P < 0.05$). B. Semi-quantitative gene expression of *Sp-IAG* in different tissues of female crabs using RT-PCR. C. Western blot analysis of Sp-IAG in the reproductive system of male crabs. AG: androgenic gland; SV: seminal vesicle; ED: ejaculatory duct; Br: brain; TG: thoracic ganglion; Es: eyestalk.

the control, no green fluorescence was detected (Fig. 3). This result indicated that Sp-IAG existed endogenously in the AG, which is consistent with previously reported results (Li et al., 2012).

3.6. Effects of mating on Sp-IAG expression

Real-time PCR showed that *Sp-IAG* expression increased significantly after mating (Fig. 4). As is reported in previous research, AG is more active in the mating season and the size of the AG increased and the cell type of the AG changed (Liu et al., 2008). Our result demonstrated that the AG's activity was related to mating at gene level. It further verified that the AG and its representative gene, *Sp-IAG*, were vital to mating and reproduction.

3.7. Effects of eyestalk ablation on Sp-IAG expression

Real-time PCR showed that *Sp-IAG* expression is notably elevated in bilateral eyestalk-ablated crabs after 3 and 7 days in the AG (Fig. 5A), and in the ED (Fig. 5B). However, the expression in the SV was not similar, and showed that the *Sp-IAG* expression in the SV remained the same in the control and eyestalk-ablation groups (data not shown). *Sp-IAG* expression in the control groups was not identical, perhaps as a result of the crabs that we used not being at coincident developmental stages.

4. Discussion

In the noncommittal sexual determination and differentiation of crustaceans, it is well known that the AG plays a vital role in male sexual differentiation and maintaining sexual characteristics. The inhibitory effects of the AG on ovarian development in the mud crab *S. paramamosain* were investigated in order to develop a bioassay for the androgenic hormone (Cui et al., 2005), and the cell structure and seasonal changes of the AG of the mud crab were studied several years later (Liu et al., 2008). In this paper, an AG-specific expressed gene from the *S. paramamosain* AG was identified and named as *Sp-IAG*.

Sp-IAG cDNA (1289 bp) is longer than *Cas-IAG* cDNA (1126 bp) (Chung et al., 2011) and *Pp-IAG* (923 bp) (Sroyraya et al., 2010), and the predicted ORF of *Sp-IAG* was similar to that of other IAGs found in crustaceans (Chung et al., 2011; Li et al., 2012; Manor et al., 2007; Ohira et al., 2003; Okuno et al., 1999; Ventura et al., 2009). Based on the disulfide assignments reported in decapod and isopod AGHs (Chung et al., 2011; Martin et al., 1999), two interdisulfide bridges were formed between the B and A chains and one intradisulfide bridge in the A chain. Two proteolytic motifs (RYKR/RFRR) existing in other decapods and isopods can be found in Sp-IAG (Manor et al., 2007; Okuno et al., 1999; Ventura et al., 2009). In addition, a putative N-linked glycosylated site "NCT" was found in A chain, which is a common post-translational marker of regulated protein function and activity, and the diversity of life. The N-linked glycosylated site is also found in three AGHs in isopods, *Cq-IAG*, *Fc-IAG1* and *Fc-IAG2*, which is common in IAGs (Li et al., 2012; Manor et al., 2007).

Sp-IAG 5′ flanking sequence contains many putative transcription factor binding sites, which offers more information about this gene's function, such as CRE-BP, C/EBPbeta, Cyclin A1, GATA1, CAP, Dfd, and SRY. A GC box is also found in the 5′ flanking sequence which is deemed a cis-acting transcriptional regulatory element and would play an important role in assembling transcription complexes on promoters to enhance gene's expression (Klug et al., 2009). SRY (sex-determining region Y) is a sex-determining gene on the Y chromosome, since its discovery, the importance of the SRY gene in sex determination has been extensively documented (Wallis et al., 2008; Whitfield et al., 1995). The existence of putative SRY transcription factors indicated that *Sp-IAG* was indeed relevant to male sexual development. Furthermore, it was confirmed that GATA-1 modulated testis-specific expression of mouse cyclin A1 (Panigrahi et al., 2012). Cyclin A1 is a male germ cell-specific cell cycle regulator that is essential for spermatogenesis (Liu et al., 1998; Panigrahi et al., 2012). Thus, GATA-1 found in 5′ flanking sequence may illustrate that *Sp-IAG* may be related to spermatogenesis. Existence of putative binding sites for these transcription factors in the 5′ flanking sequence implied a possible regulation manner on transcription level of *Sp-IAG* gene, and contributed to further investigate the regulation of this gene.

The functions of AGs have been the subject of research for many years, and it is widely accepted that the AG is closely related to male sex differentiation and maintaining sexual characteristics. More and

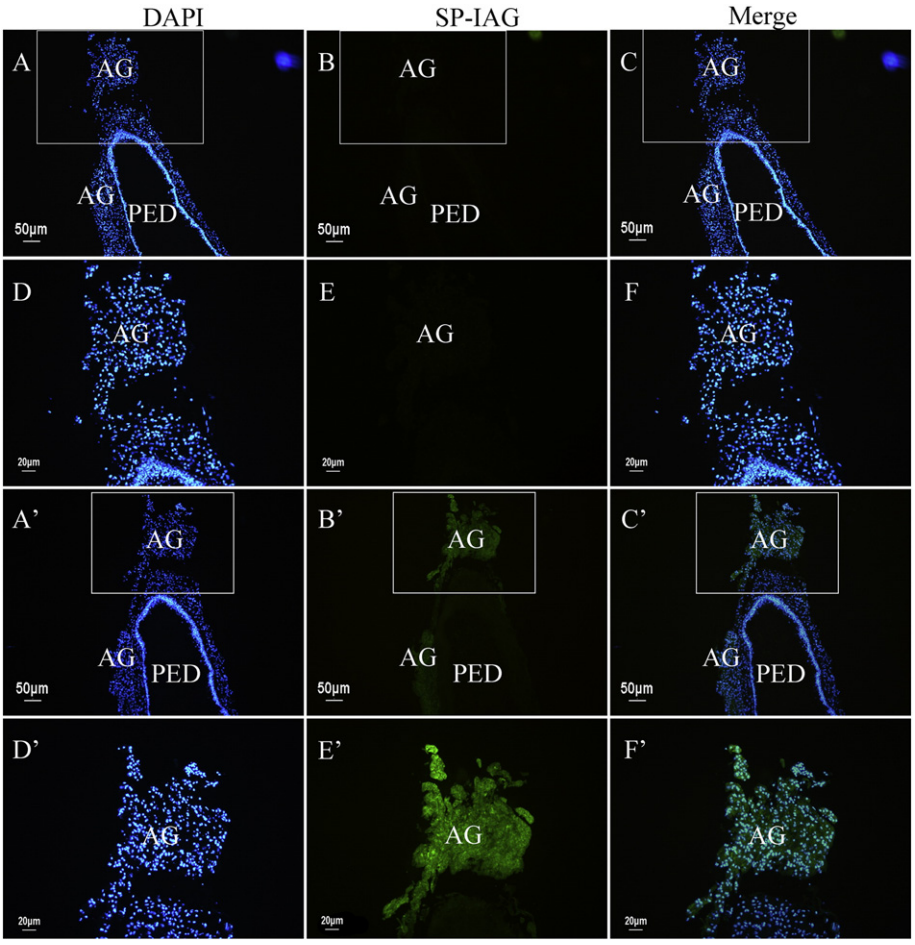

Fig. 3. Immunofluorescence analysis of PED. Panels A–F are immunofluorescence staining of posterior ejaculatory duct treated with pre-immune serum. Panels D, E, and F are higher magnification of positive signal areas in panels A, B, and C. Panels A′–F′ are immunofluorescence staining of posterior ejaculatory duct treated with Sp-IAG antibody. Panels D′, E′, and F′ are higher magnification of positive signal areas in panels A′, B′, and C′. AG: androgenic gland, PED: posterior ejaculatory duct.

more studies reveal that AG not only functions as a reproductive regulator, but also shows involvement in the rate of growth. Therefore, the AG's role is similar to that of IGF, a member of the insulin superfamily (Sagi and Khalaila, 2001). Real-time PCR showed that *Sp-IAG* was present not only in the ED and SV, but also in the AG as previously reported (Manor et al., 2007; Okuno et al., 1999; Sroyraya et al., 2010; Ventura et al., 2009). Phoungpetchara et al. (2011) suggest that Mr-IAG was secreted and transported from the AG to the testis, spermatic duct and ejaculatory bulb epithelium, perhaps through the interconnecting hemolymph vessels between the three organs, but they detect the protein only in the AG, not in the testis, spermatic duct or ejaculatory bulb. It is the first time to detect IAG protein in seminal vesicle and the content is very high, we speculated that Sp-IAG probably has some effect on controlling the function of the seminal vesicle involved in sperm transport. No *Sp-IAG* was detected in female tissues, which offered sufficient evidence that Sp-IAG played critical roles in the male reproductive process.

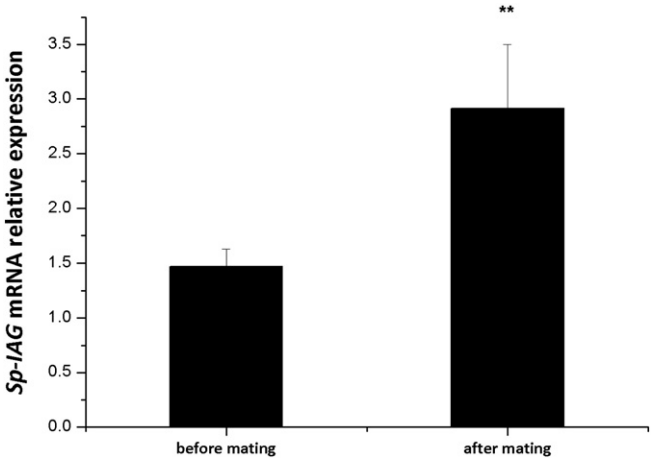

Fig. 4. Relative gene expression of *Sp-IAG* in the androgenic gland after mating detected using real-time PCR. The data presented includes the mean and standard error of the mean derived from triplicate experiments (*$P < 0.05$).

Liu (Liu et al., 2008) studies the seasonal changes in morphology and histology of the androgenic gland in the mud crab *S. paramamosain*. During the mating season, the AG in *S. paramamosain* was most active and reached its maximum size. Devi and Smija (2014) investigated the seasonal variation in the structure and secretory activity of the androgenic gland in the freshwater crab *Travancoriana schirnerae*, and found that the secretory activity was almost completed by the mating time with type II cells. Similarly observed in our study, the *Sp-IAG* expression was increased significantly after mating, which demonstrated that AG's activity was increased during mating at gene level.

In the present study, *Sp-IAG* mRNA transcripts were elevated drastically both in the AG and ED after ESA, which suggested that the elevation might have resulted from the reduction of inhibitory substances on the AG produced by the XO–SG (Chung et al., 2011). ESA has been widely used in the aquaculture of crustacean economic species industry. ESA

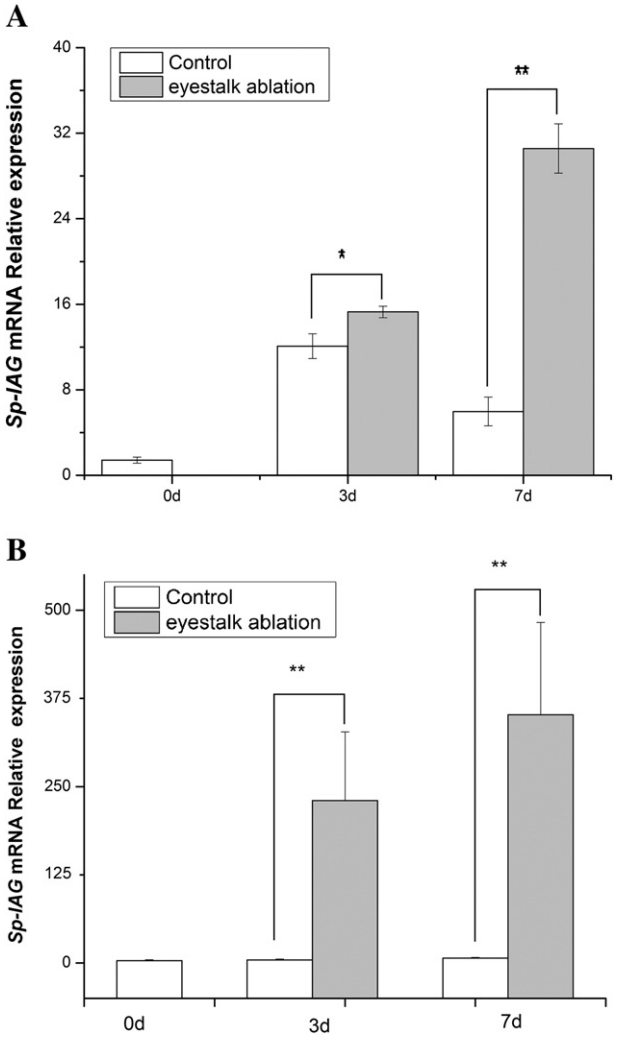

Fig. 5. A. Relative gene expression of *Sp-IAG* in the androgenic gland after eyestalk ablation was detected using real-time PCR. The data presented includes the mean and standard error of the mean derived from triplicate experiments (*$P < 0.05$). B. Relative gene expression of *Sp-IAG* in the ejaculatory duct after eyestalk ablation was detected using real-time PCR. The data presented includes the mean and standard error of the mean derived from triplicate experiments (*$P < 0.05$).

can lead to sexual precocity, since, in the shrimp *Penaeus canaliculatus*, ESA females spawn more frequently than intact females (Choy, 1987). Similarly in the black tiger shrimp, growth rates (length and body weight), ovary weight and gonadosomatic index of the female shrimp significantly increase after ESA (Uawisetwathana et al., 2011). ESA also has an effect on activity of AG. In *C. quadricarinatus*, ESA causes an increase in the AG weight and overexpression of AG polypeptides (Khalaila et al., 2002). ESA affects the scale of the AG cell types in the blue swimmer crab, *P. pelagicus*, as implied by an altered ability to synthesize the insulin-like AGH. Specific elevation of IAG expression following eyestalk removal in the blue crab *C. sapidus* is reported (Chung et al., 2011), which is consistent with our study. Male eyestalk ablation can increase gonad size and double mating frequency of *Penaeus vannamei* (Chamberlain and Lawrence, 1981). Gonad inhibitory hormone (GIH) which produced in XO–SG in the eyestalk apparently occurs in nature in the non-breeding season and is absent or present only in low levels during the breeding season. Thus, eyestalk ablation is an effective technique for removing the inhibitory effect on AG that produced by XO–SG and artificial induction of maturation. However, mating is under the natural breeding season when GIH is also at low level. Sp-IAG expression was increased significantly after eyestalk ablation and mating, which showed the same effects on maturation of male *S. paramamosain* of both modes.

In summary, our study characterized a new insulin-like gene found in the AG of the mud crab, *S. paramamosain*, and predicted its structure via deduced amino acids. Our results confirmed IAG's vital functions in sexual differentiation and maintaining male characters in crustaceans. ESA experiments verified the existence of the eyestalk–AG–testis axis in *S. paramamosain*. Our research, which provided the theoretical basis for elucidating the mechanism of sex differentiation of crustaceans, also has potential practical value.

Supplementary data to this article can be found online at http://dx.doi.org/10.1016/j.aquaculture.2014.06.033.

Acknowledgments

This work was supported by grants (U1205123, 41176116) from the National Natural Science Foundation of China (NSFC), and by a grant (2012N0029) from the Fujian Science and Technology Department. Professor John Hodgkiss is thanked for his help with the English language.

References

Barki, A., Karplus, I., Manor, R., Sagi, A., 2006. Intersexuality and behavior in crayfish: the de-masculinization effects of androgenic gland ablation. Horm. Behav. 50, 322–331.
Chamberlain, G.W., Lawrence, A.L., 1981. Effect of light intensity and male and female eyestalk ablation on reproduction of *Penaeus stylirostris* and *P. vannamei*. J. World Maricult. Soc. 12 (2), 357–372.
Charniaux-Cotton, H., 1954. Discovery in, an amphipod crustacean (*Orchestia gammarella*) of an endocrine gland responsible for the differentiation of primary and secondary male sex characteristics. C.R. Hebd. Seances Acad. Sci. 239, 780–782.
Choy, S.C., 1987. Growth and reproduction of eyestalk ablated *Penaeus canaliculatus* (Olivier, 1811) (crustacea: Penaeidae). J. Exp. Mar. Biol. Ecol. 112, 93–107.
Chung, J.S., Manor, R., Sagi, A., 2011. Cloning of an insulin-like androgenic gland factor (IAG) from the blue crab, *Callinectes sapidus*: implications for eyestalk regulation of IAG expression. Gen. Comp. Endocrinol. 173, 4–10.
Cronin, L.E., 1947. Anatomy and histology of the male reproductive system of *Callinectes sapidus* Rathbun. J. Morphol. 81, 209–239.
Cui, Z.X., Liu, H., Lo, T.S., Chu, K.H., 2005. Inhibitory effects of the androgenic gland on ovarian development in the mud crab *Scylla paramamosain*. Comp. Biochem. Physiol. A 140, 343–348.
Devi, A.R., Smija, M.K., 2014. Seasonal changes in the structure and secretory activity of the androgenic gland of *Travancoriana schirnerae*. Cent. Eur. J. Biol. 9 (1), 70–79.
Eastman-Reks, S., Fingerman, M., 1984. Effects of neuroendocrine tissue and cyclic AMP on ovarian growth in vivo and in vitro in the fiddler crab, *Uca pugilator*. Comp. Biochem. Physiol. A 79, 679–684.
Hoffman, D.L., 1968. Seasonal eyestalk inhibition on the androgenic glands of a protandric shrimp. Nature 218, 170–172.
Hunter, G.A., Donaldson, E.M., Stoss, J., Baker, I., 1983. Production of monosex female groups of chinook salmon (*Oncorhynchus tshawytscha*) by the fertilization of normal ova with sperm from sex-reversed females. Aquaculture 33, 355–364.
Jensen, G., Shelton, W., 1979. Effects of estrogens on *Tilapia aurea*: implications for production of monosex genetic male tilapia. Aquaculture 16, 233–242.
Katakura, Y., 1960. Transformation of ovary into testis following implantation of androgenous glands in *Armadillidium vulgare*, an isopod crustacean. Annot Zool Jpn. 33, 241–244.
Khalaila, I., Katz, T., Abdu, U., Yehezkel, G., Sagi, A., 2001. Effects of implantation of hypertrophied androgenic glands on sexual characters and physiology of the reproductive system in the female red claw crayfish, *Cherax quadricarinatus*. Gen. Comp. Endocrinol. 121, 242–249.
Khalaila, I., Manor, R., Weil, S., Granot, Y., Keller, R., Sagi, A., 2002. The eyestalk–androgenic gland–testis endocrine axis in the crayfish *Cherax quadricarinatus*. Gen. Comp. Endocrinol. 127, 147–156.
Klug, W.S., Cummings, M.R., Spencer, C.A., Palladina, M.A., 2009. Concepts of Genetics, Ninth ed. Pearson Benjamin Cummings, San Francisco.
Li, S., Li, F., Sun, Z., Xiang, J., 2012. Two spliced variants of insulin-like androgenic gland hormone gene in the Chinese shrimp, *Fenneropenaeus chinensis*. Gen. Comp. Endocrinol. 177, 246–255.
Liu, D., Matzuk, M.M., Sung, W.K., Guo, Q., Wang, P., Wolgemuth, D.J., 1998. Cyclin A1 is required for meiosis in the male mouse. Nat. Genet. 20, 377–380.
Liu, H., Cheung, K.C., Chu, K.H., 2008. Cell structure and seasonal changes of the androgenic gland of the mud crab *Scylla paramamosain* (Decapoda: Portunidae). Zool. Stud. 47, 720–732.
Ma, K.Y., Lin, J.Y., Guo, S.Z., Chen, Y., Li, J.L., Qiu, G.F., 2013. Molecular characterization and expression analysis of an insulin-like gene from the androgenic gland of the oriental river prawn, *Macrobrachium nipponense*. Gen. Comp. Endocrinol. 185, 90–96.
Malecha, S.R., Nevin, P.A., Ha, P., Barck, L.E., Lamadrid-Rose, Y., Masuno, S., Hedgecock, D., 1992. Sex-ratios and sex-determination in progeny from crosses of surgically sex-

reversed freshwater prawns, *Macrobrachium rosenbergii*. Aquaculture 105, 201–218.
Manor, R., Aflalo, E.D., Segall, C., Weil, S., Azulay, D., Ventura, T., Sagi, A., 2004. Androgenic gland implantation promotes growth and inhibits vitellogenesis in *Cherax quadricarinatus* females held in individual compartments. Invertebr. Reprod. Dev. 45, 151–159.
Manor, R., Weil, S., Oren, S., Glazer, L., Aflalo, E.D., Ventura, T., Chalifa-Caspi, V., Lapidot, M., Sagi, A., 2007. Insulin and gender: an insulin-like gene expressed exclusively in the androgenic gland of the male crayfish. Gen. Comp. Endocrinol. 150, 326–336.
Martin, G., Sorokine, O., Moniatte, M., Bulet, P., Hetru, C., Van Dorsselaer, A., 1999. The structure of a glycosylated protein hormone responsible for sex determination in the isopod, *Armadillidium vulgare*. Eur. J. Biochem. 262 (3), 727–736.
Nagamine, C., Knight, A.W., 1987. Masculinization of female crayfish, *Procambarus clarki* (Girard). Int. J. Invertebr. Reprod. Dev. 11, 77–87.
Nagamine, C., Knight, A.W., Maggenti, A., Paxman, G., 1980. Masculinization of female *Macrobrachium rosenbergii* (de Man) (Decapoda, Palaemonidae) by androgenic gland implantation. Gen. Comp. Endocrinol. 41, 442–457.
Ohira, T., Hasegawa, Y., Tominaga, S., Okuno, A., Nagasawa, H., 2003. Molecular cloning and expression analysis of cDNAs encoding androgenic gland hormone precursors from two Porcellionidae species, *Porcellio scaber* and *P. dilatatus*. Zool. Sci. 20, 75–81.
Okuno, A., Hasegawa, Y., Ohira, T., Katakura, Y., Nagasawa, H., 1999. Characterization and cDNA cloning of androgenic gland hormone of the terrestrial isopod *Armadillidium vulgare*. Biochem. Biophys. Res. Commun. 264, 419–423.
Ōtsu, T., 1963. Bihormonal control of sexual cycle in the freshwater crab, *Potamon dehaani*. Embryologia 8, 1–20.
Panigrahi, S.K., Vasileva, A., Wolgemuth, D.J., 2012. Sp1 transcription factor and GATA1 cis-acting elements modulate testis-specific expression of mouse cyclin A1. PLoS One 7, e47862.
Phoungpetchara, I., Tinikul, Y., Poljaroen, J., Chotwiwatthanakun, C., Vanichviriyakit, R., Sroyraya, M., Hanna, P.J., Sobhon, P., 2011. Cells producing insulin-like androgenic gland hormone of the giant freshwater prawn, *Macrobrachium rosenbergii*, proliferate following bilateral eyestalk-ablation. Tissue Cell 43 (3), 165–177.
Puckett, D.H., 1964. Experimental studies on the crayfish androgenic gland in relation to testicular function(PhD dissertation) University of Virginia.
Sagi, A., Khalaila, I., 2001. The crustacean androgen: a hormone in an isopod and androgenic activity in decapods. Am. Zool. 41, 477–484.
Sagi, A., Cohen, D., Milner, Y., 1990. Effect of androgenic gland ablation on morphotypic differentiation and sexual characteristics of male freshwater prawns, *Macrobrachium rosenbergii*. Gen. Comp. Endocrinol. 77, 15–22.
Singh, A.K., 2012. Introduction of modern endocrine techniques for the production of monosex population of fishes. Gen. Comp. Endocrinol. 181, 146–155.
Sroyraya, M., Chotwiwatthanakun, C., Stewart, M.J., Soonklang, N., Kornthong, N., Phoungpetchara, I., Hanna, P.J., Sobhon, P., 2010. Bilateral eyestalk ablation of the blue swimmer crab, *Portunus pelagicus*, produces hypertrophy of the androgenic gland and an increase of cells producing insulin-like androgenic gland hormone. Tissue Cell 42, 293–300.
Suzuki, S., Yamasaki, K., 1997. Sexual bipotentiality of developing ovaries in the terrestrial isopod *Armadillidium vulgare* (Malacostraca, Crustacea). Gen. Comp. Endocrinol. 107, 136–146.
Taketomi, Y., Nishikawa, S., 1996. Implantation of androgenic glands into immature female crayfish, *Procambarus clarkii*, with masculinization of sexual characteristics. J. Crustac. Biol. 16, 232–239.
Uawisetwathana, U., Leelatanawit, R., Klanchui, A., Prommoon, J., Klinbunga, S., Karoonuthaisiri, N., 2011. Insights into eyestalk ablation mechanism to induce ovarian maturation in the black tiger shrimp. PLoS One 6, e24427.
Ventura, T., Sagi, A., 2012. The insulin-like androgenic gland hormone in crustaceans: from a single gene silencing to a wide array of sexual manipulation-based biotechnologies. Biotechnol. Adv. 30, 1543–1550.
Ventura, T., Manor, R., Aflalo, E.D., Weil, S., Raviv, S., Glazer, L., Sagi, A., 2009. Temporal silencing of an androgenic gland-specific insulin-like gene affecting phenotypical gender differences and spermatogenesis. Endocrinology 150, 1278–1286.
Wallis, M.C., Waters, P.D., Graves, J.A.M., 2008. Sex determination in mammals — before and after the evolution of SRY. Cell. Mol. Life Sci. 65, 3182–3195.
Whitfield, L.S., Hawkins, T.L., Goodfellow, P.N., Sulston, J., 1995. 41 kilobases of analyzed sequence from the pseudoautosomal and sex-determining regions of the short arm of the human Y chromosome. Genomics 27, 306–311.